

A liquid crystal spatial light phase modulator and its applications

Tsutomu Hara

Central Research Laboratory; Hamamatsu Photonics K.K.

5000 Hirakuchi, Hamakita-City, Shizuoka-Prefecture, 434-8601 JAPAN ,

TEL: +81-53-586-7111; FAX: +81-53-586-6180; E-mail: hara@crl.hpk.co.jp

ABSTRACT

We have developed optically-addressed and electrically-addressed liquid crystal spatial phase-only light modulators without pixelized structures. We obtained a large depth of phase-only modulation based on the electro-optical characteristics of a parallel-aligned nematic liquid crystal. We also confirmed that the satisfactory phase modulation capability and high diffraction efficiency of these spatial light modulators were useful for practical applications such as optical correlation, holographic measurement, optical waveform shaping, and optical wavefront compensation.

Keywords: Spatial light modulator, Optical information processing, Phase modulation, Optical waveform shaping, Optical wavefront compensation, Adaptive optics, Vibration measurement

1. INTRODUCTION

Two-dimensional phase-only light modulation has aroused a great deal of interest in many areas, such as optical correlation, optical interconnection, optical manipulation, laser processing, adaptive optics and holographic measurement. As a result, there is a strong call for a spatial phase-only light modulator for these applications.

A liquid crystal display (LCD) is easily and inexpensively available as a commercial component, so it has been utilized for studies as a phase modulator. However, most LCDs cannot at present achieve the real 2π radian phase-only modulation which is required for many applications. Furthermore, they involve unavoidable drawbacks, such as energy loss caused by a limited aperture size and diffraction noise caused by a pixelized structure.

In order to provide a practical device, we developed a nonpixelized, optically-addressed, parallel-aligned nematic-liquid-crystal spatial light modulator (PAL-SLM)¹⁾. We obtained a large depth of phase-only modulation based on the electro-optical characteristics of a parallel-aligned nematic-liquid-crystal layer.

Moreover, the phase-only modulator must be controlled by a computer if it is to produce real-time displays of computer-created patterns. We therefore developed a nonpixelized electrically-addressable spatial light phase-only modulator^{2,3)}. The device consists of a PAL-SLM, coupling optics, an XGA liquid crystal display (LCD), a laser diode (LD) and collimating optics.

These characteristics of spatial light modulators are useful for many practical applications. We present the latest advance in applications research using spatial light modulators.

2. PAL-SLM

The structure of a PAL-SLM is shown in Fig.1 and a photograph of it is shown in Fig.2. The device is an optically-addressed spatial light modulator which has a sandwich structure consisting of a hydrogenated amorphous silicon (a-Si:H) photoconductive layer used for addressing, a dielectric mirror, and a parallel-aligned nematic liquid crystal layer used for modulating between the two transparent conductive electrodes (ITO). The effective area is 20mm \times 20mm. Figure 3 shows the operating principle of the device. A driving voltage is applied to the ITO electrodes. Illuminating the a-Si:H layer with write-in light supplies a voltage to the liquid crystal layer. This causes the liquid crystal molecules to tilt, so that the refractive index of the liquid crystal layer is changed and the readout light is modulated with the write-in light information.

The transfer characteristic (the relationship between the write-in light intensity and the phase shift of the readout light) of the device is shown in Fig.4. We used an LD at a wavelength of 680nm for both the write-in light and the readout light. A phase shift of more than 2π radians can be achieved with a write-in light intensity of $200\mu\text{W}/\text{cm}^2$ when applying a voltage of 3.0V and using a readout laser light polarized in parallel to the molecular axis of the liquid crystal. A response time of 30msec was measured when the phase modulation depth was π radians.

Figure 5 shows the diffraction efficiency of the device. At low spatial frequencies (<5 line pairs/mm), the diffraction efficiency was 31%, which was very close to the theoretical maximum for Raman-Nath diffraction (33.9%).

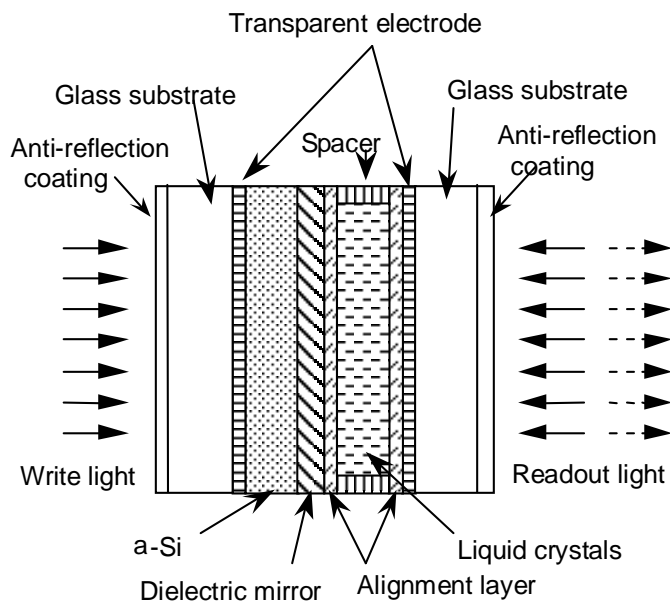


Fig.1 Structure of a PAL-SLM.

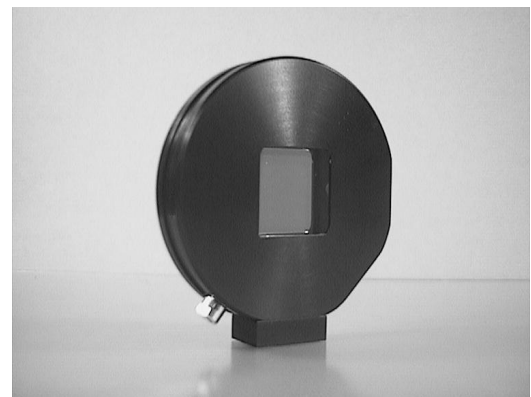


Fig.2 Photograph of a PAL-SLM.

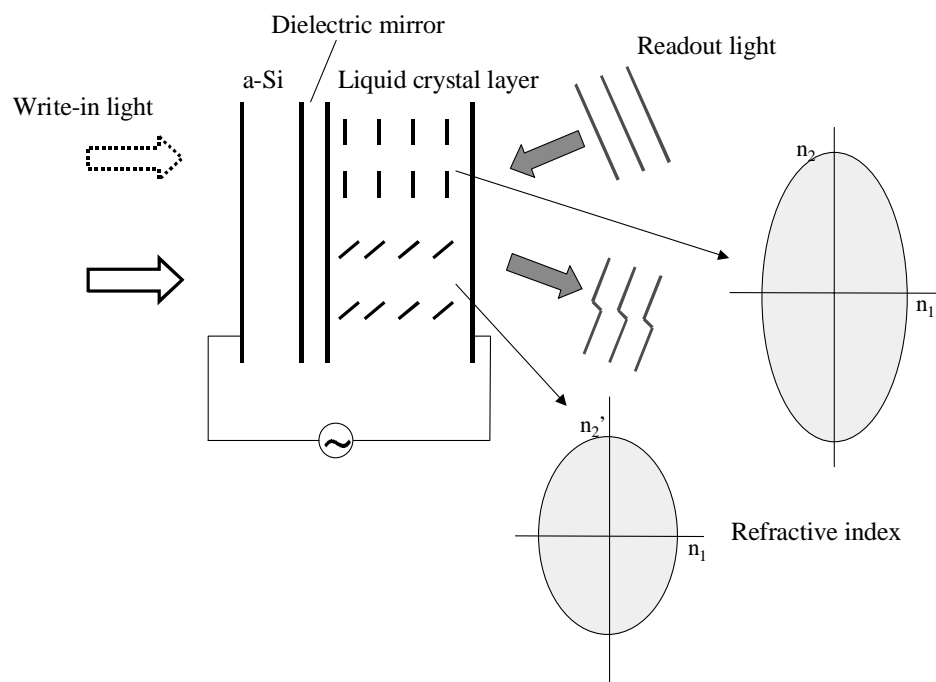


Fig.3 Operating principle of a PAL-SLM.

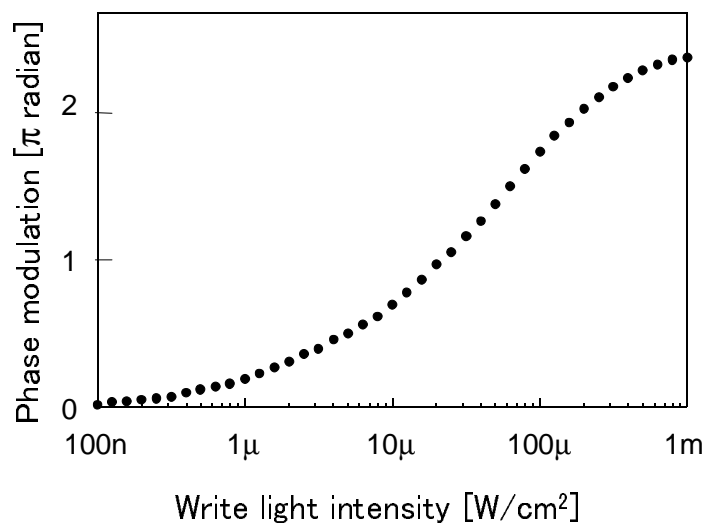


Fig.4 Transfer characteristic of a PAL-SLM.

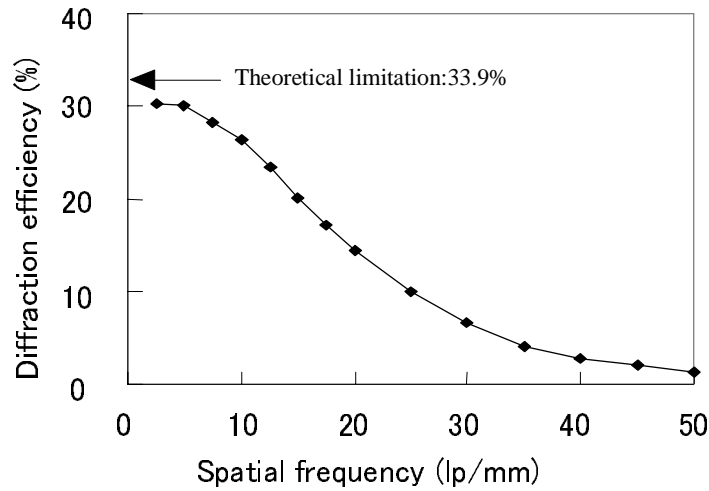


Fig.5 Diffraction efficiency of a PAL-SLM.

3. LCD coupled PAL-SLM module

The LCD coupled PAL-SLM module is an electrically-addressed spatial light modulator that allows easy computer-controlled pixel manipulation while producing images comprising continuous pixels. The module consists of an XGA-LCD (Sony) having 1024×768 pixels, a coupling lens, a PAL-SLM, a laser diode (LD) used to illuminate the LCD and collimating optics for the LD. We designed a new set of coupling lenses so as not to transfer the pixel structure of the LCD.

The experimental setup used to study the phase modulation characteristics of the device is shown in Fig.6. The write-in pattern was written in the LCD by means of serial electrical signals, and transferred to the PAL-SLM by means of an LD (680nm) used as the writing light source. And we used an LD at a wavelength of 680nm for a readout light. We also applied an oblique incident readout light. The oblique readout configuration make it possible for an optical system to avoid power loss in the readout light.

The readout images are shown in Fig.7, where (a), (b) and (c) represent an output image of the LCD alone, an image of the module at π radian modulation and that image at a phase modulation of 2π radians, respectively. The pixelized structure was eliminated in Fig.7(b). It was also observed in Fig.7(b) that the signals having the highest spatial frequency (upper left) were transferred effectively. Figure 7(c) shows that a phase modulation depth of 2π radians was obtained.

Figures 8(b) and (c) show the Fourier transformed patterns of a fingerprint image (a). Surplus diffraction light (diffraction noise) caused by the pixel structure was reduced to less than 3% by means of the coupling optics (Fig.8(c)), as compared to almost 50% occurring in the LCD itself (Fig.8(b)).

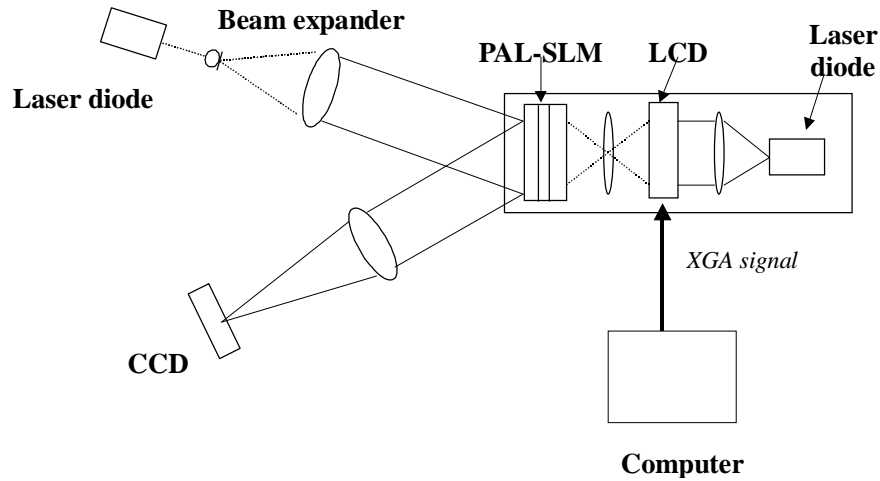


Fig.6 Experimental setup used to measure module performance.

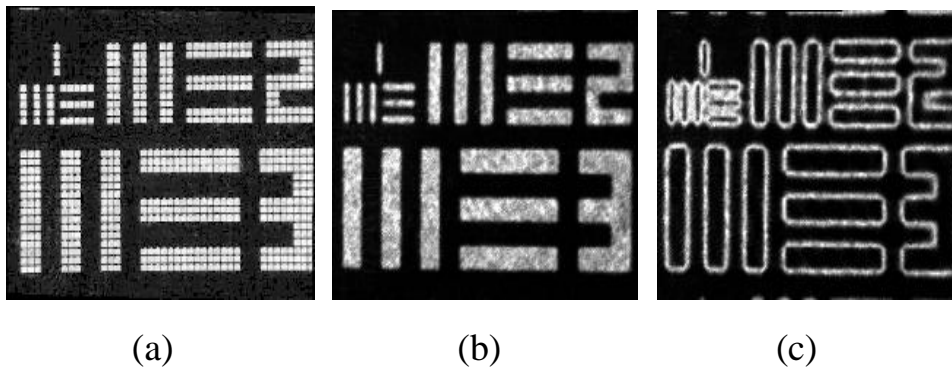


Fig.7 Readout images: (a)output image of the LCD itself; (b)output image of the module at π radian phase modulation; (c)output image of the module at 2π radian phase modulation.

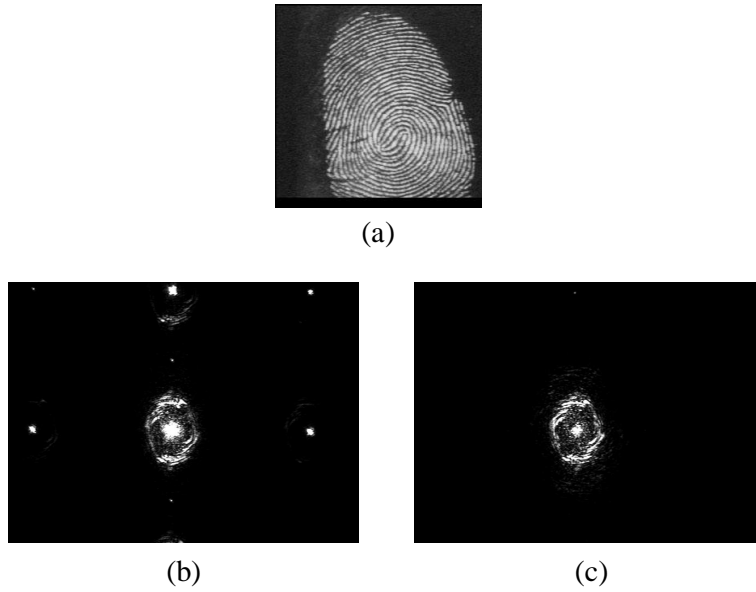


Fig.8 Fourier transformed images: (a)input fingerprint image; (b)Fourier transformed image of the LCD itself; (c)Fourier transformed image of the module.

The module makes it possible to achieve linearization of transfer characteristics by calibrating and adjusting the transfer characteristics of an LCD and PAL-SLM that are not linear originally. The transfer characteristic of the module was measured. Uniform patterns of each gray level were displayed on the LCD and the amount of phase modulation of the PAL-SLM was measured as a function of the gray level. The relationship between phase modulation and gray level was almost linear, and a modulation of more than 2π radians was achieved, as shown in Fig.9.

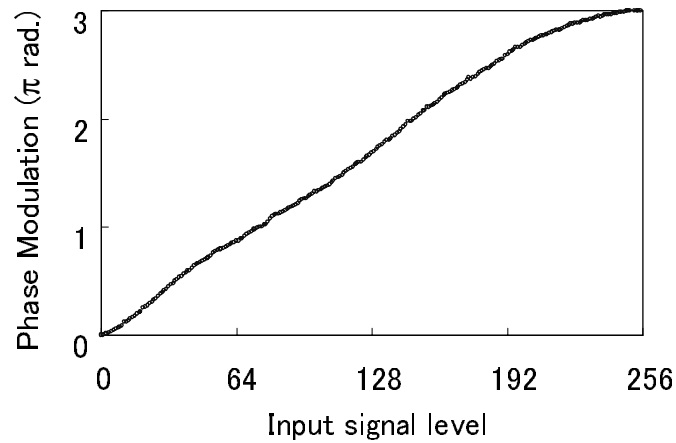


Fig.9 Linearized transfer characteristic of the module.

The diffraction efficiency of the device was also measured. In the case of a binary $(0, \pi)$ grating, the theoretical value of the diffraction efficiency is 40.5%. A higher diffraction efficiency can be obtained by using a multi-level grating. For example, the diffraction efficiency of a four-level $(0, 0.5\pi, \pi, 1.5\pi)$ grating is theoretically 76%. Figure 10 shows the diffraction efficiency of the device, which exceeds 35% at a spatial frequency of 10 lp/mm for a binary $(0, \pi)$ grating. When a multilevel $(0, 0.5\pi, \pi, 1.5\pi)$ grating was written in the device, a diffraction efficiency of more than 70% was obtained at a spatial frequency of 10 lp/mm.

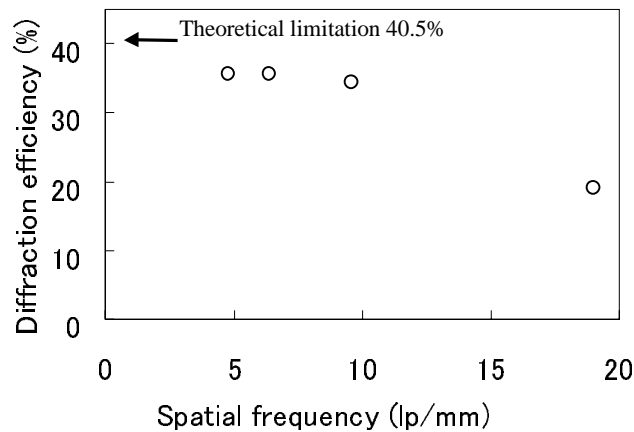


Fig.10 Diffraction efficiency for a binary grating of the module.

4. APPLICATIONS

(1) Optical computing

We designed and constructed the compact Joint Transform Correlator (JTC) system^{4,5)} shown in Fig.11. It consists of a liquid crystal display (SLM1) used to display the input image, two Fourier transforming lenses, a PAL-SLM (SLM2) in the joint Fourier transform plane, a CCD camera used to detect the correlation signal, and a laser diode (LD) serving as the readout light source. Parallel optical processing makes it possible for the system to provide a correlation signal in less than 0.1 second for an input image of $512 \times 512 \times 8$ bits. As a first step, we applied the correlator to fingerprint identification.

(2) Holographic measurement

Vibration measurements based on holographic techniques are essential to visualize the vibration patterns of rough surfaces. Recently, these techniques were applied to the vibration analysis of musical and mechanical instruments, as well as to car body vibration measurements. We applied the time-average method to vibration measurements of rough surfaces in near-real time using the PAL-SLM as recording material⁶⁾.

Figure 12 shows the optical arrangement used for vibration measurements. The beam from an He-Ne laser was collimated, and illuminated a vibrating object at an angle θ smaller than 10° between the vibrating surface and the beam. The vibrating surface was imaged onto the PAL-SLM. The reference beam was introduced into the PAL-SLM. The two beams interfered with each other and produced a holographic image of the vibrating object that was recorded in the PAL-SLM. Another He-Ne laser was used to read-out the PAL-SLM. The reconstructed image was observed using a CCD camera. Figure 13 shows the experimental results. We easily observed the vibration pattern in near-real time while changing the vibration frequency.

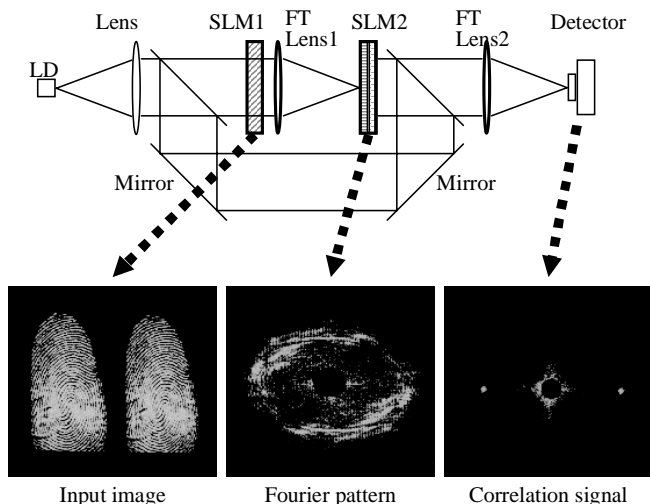


Fig.11 Optical correlator for fingerprint identification.

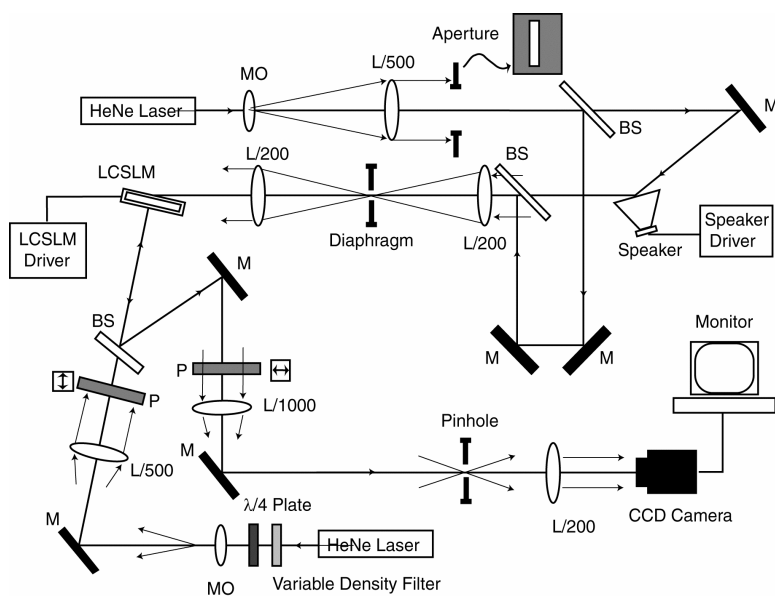


Fig.12 Optical arrangement used for vibration measurements.

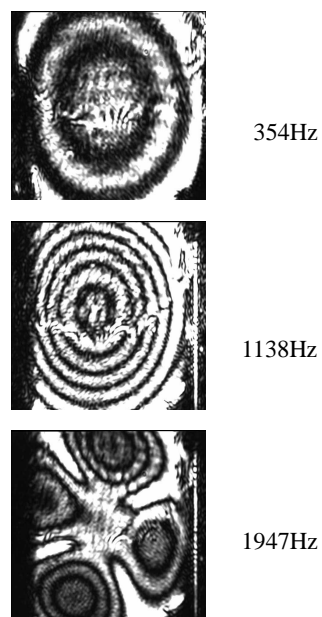


Fig.13 Vibration pattern of a rough surface at different frequencies.

(3) Optical waveform shaping

Figure 14 shows the experimental results of laser waveform shaping. For this application a computer generated hologram (CGH) was designed using a computer, and written into the SLM. The readout light was modulated in the SLM as designed. A Gaussian-shaped beam from a laser could be changed into a circular shaped beam, a rectangular shaped beam, a star shaped beam etc. without energy loss. This technology can be applied to a laser processing system and a laser printing system.

(4) Optical interconnection

We implemented a reconfigurable free space optical interconnection module⁷⁾ that connects LSI chips with parallel optical input and output channels. Figure 15 shows the principle of the system. The interconnection topology can be reconfigured by modifying a computer generated hologram (CGH) written on a PAL-SLM, and located at the Fourier plane of the module. The appropriate interconnection topology can therefore be built to meet the requirements of a given application. For example, a light from an LD on an LSI chip can be transmitted to several photodiodes (PDs) simultaneously.

The CGH can also produce a large number of optical beams from a single laser beam. This technique is applied to a multi-beam optical manipulator or optical tweezers⁸⁾ to trap and move many objects varying in size from nanometers to micrometers.

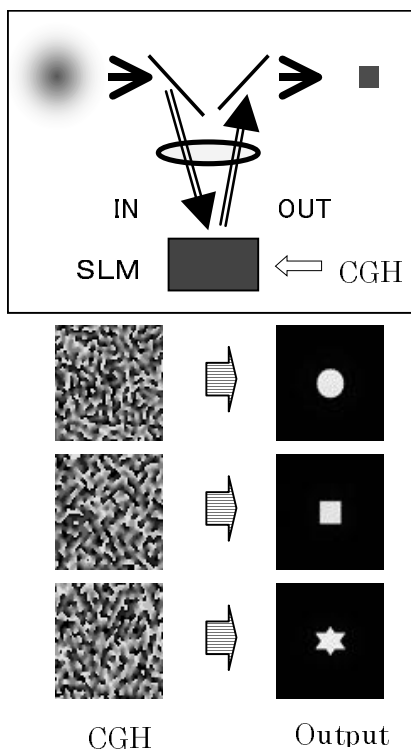


Fig.14 Laser waveform shaping.

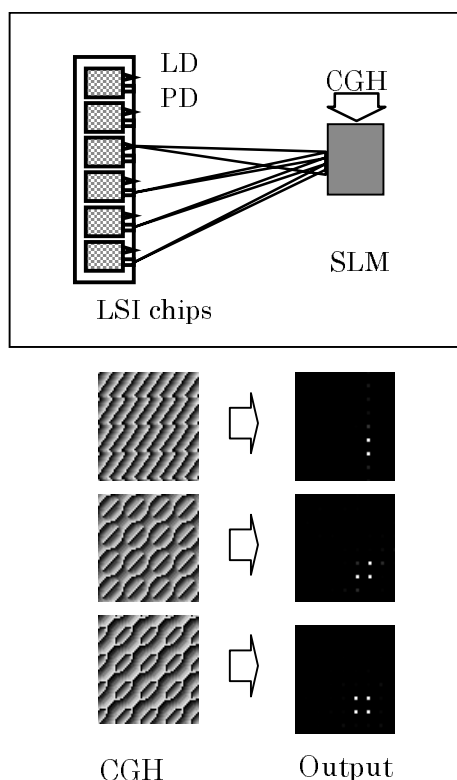


Fig.15 Reconfigurable optical interconnection.

(5) Optical wavefront compensation

Figure 16 shows the experimental system used for wavefront compensation. Distorted optical waves cannot be focused at the focal plane of a lens. By detecting the distortion using a wavefront sensor and operating the PAL-SLM using the signal from the sensor, we were able to correct the optical wavefront and focused it as shown in the photograph in Fig.17. This technique⁹⁾ can be applied to laser processing, to a telescope¹⁰⁾, and to vision science¹¹⁾ (*i.e.* ophthalmology).

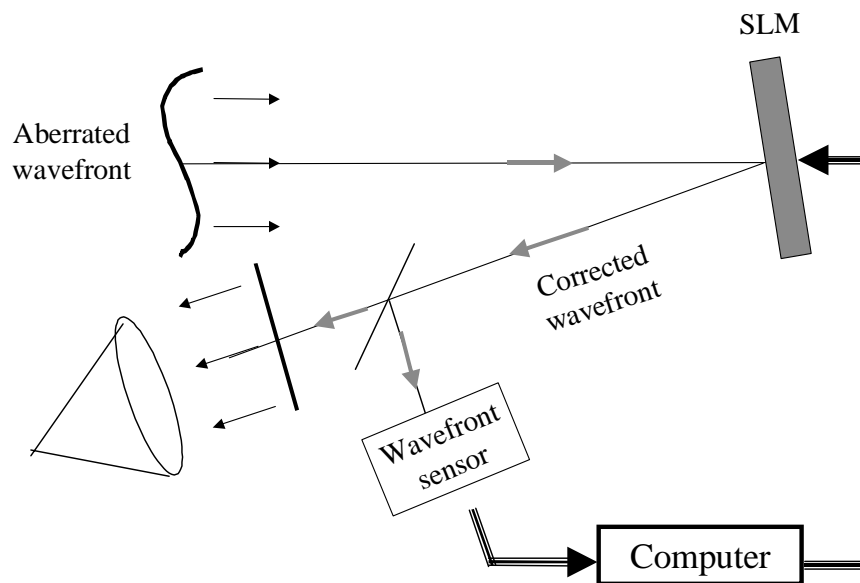


Fig.16 Optical wavefront compensation.

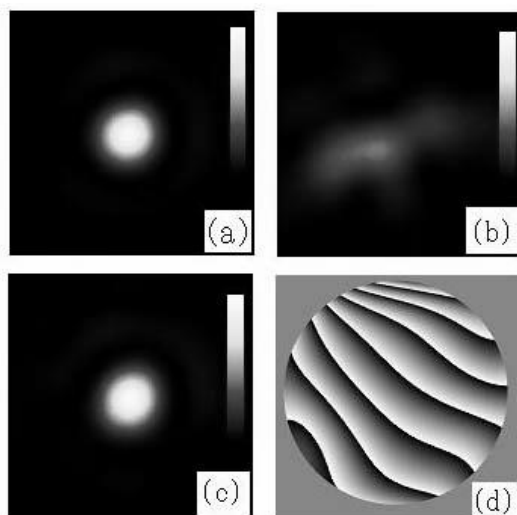


Fig.17 Experimental results of wavefront compensation: (a)no distorted beam shape; (b)distorted laser beam; (c)correction pattern; (d)corrected beam shape.

(6) Phase contrast imaging

A technique for energy-preserving phase contrast imaging has been proposed¹²⁾. The concept is based on an extension of conventional phase contrast imaging (the Zernike method) into the domain of the full range of 0 to 2π phase modulation. Figure 18 shows the proposed system¹³⁾, which was constructed using a PAL-SLM module to display a coded phase image and a PAL-SLM for phase shift filtering. An energy efficiency of 90% was confirmed experimentally. This technique has also been applied to multi-beam optical tweezers¹⁴⁾.

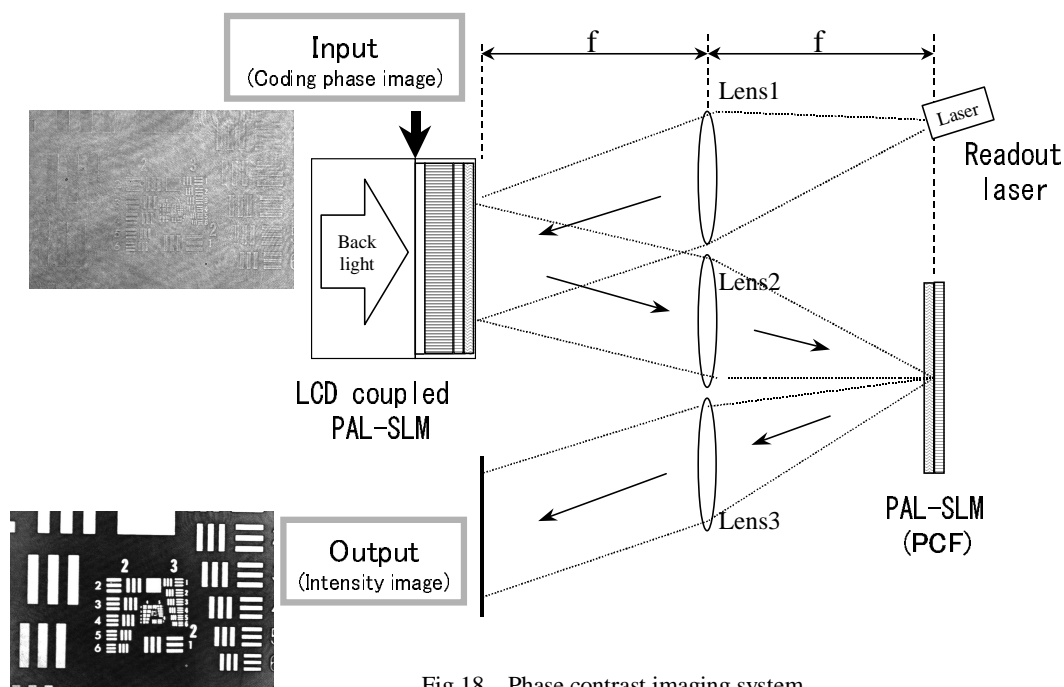


Fig.18 Phase contrast imaging system.

5. CONCLUSION

We have developed optically-addressed and electrically-addressed spatial phase-only light modulators without pixelized structures. These devices provide sufficient phase modulation capability and high diffraction efficiency. We have demonstrated that these characteristics are useful for several applications requiring two-dimensional optical phase control. Continued efforts will lead to practical applications.

ACKNOWLEDGMENT

The author would like to thank Dr.T.Hiruma and Dr.Y.Suzuki for their encouragement and support.

REFERENCES

- 1) N.Mukohzaka, N.Yoshida, H.Toyoda, Y.Kobayashi, and T.Hara, "Diffraction efficiency analysis of a parallel-aligned nematic-liquid-crystal spatial light modulator," *Appl.Opt.*, **33**, (14), pp.2804-2811 (1994).
- 2) Y.Igasaki, F.Li, N.Yoshida, H.Toyoda, T.Inoue, N.Mukohzaka, Y.Kobayashi, and T.Hara, "High Efficiency Electrically-Addressable Phase-Only Spatial Light Modulator," *Opt.Rev.*, **6**, pp.339-343 (1999).
- 3) T.Hara, N.Fukuchi, Y.Kobayashi, N.Yoshida, Y.Igasaki, and M.H.Wu, "Electrically-addressed spatial light phase modulator," *Proc.SPIE*, **4470**, p.114 (2001).
- 4) Y.Kobayashi, H.Toyoda, N.Mukohzaka, N.Yoshida, and T.Hara, "Fingerprint Identification by an Optical Joint Transform Correlation System," *Opt.Rev.*, **3**, p.403 (1996).
- 5) H.Toyoda, Y.Kobayashi, N.Mukohzaka, T.Hara, and T.Ohno, "Frame-Rate Displacement Measurement System Utilizing an Ultra-High-Speed Shutter Camera and an Optical Correlator," *IEEE Trans. Instrumentation and Measurement*, **44**, p.755 (1995).
- 6) K.Matsuda, B.Ye, N.Fukuchi, H.Okamoto, and T.Hara, "Vibration measurements of rough surfaces using an LCSLM," *ICO'04 Technical Digest*, p.411(2004).
- 7) H.Toyoda, Y.Kobayashi, N.Yoshida, Y.Igasaki, T.Hara, and M.Ishikawa, "High efficiency electrically-addressable spatial light modulator for reconfigurable optical interconnection," *OSA Snowmass Meeting, SLM'99 Technical Digest, SMB3*(1999).
- 8) J.E.Curtis, B.A.Coss, and D.G.Grier, "Dynamic holographic optical tweezers," *Opt.Commun.*, **207**, p.169 (2002).
- 9) T.Shirai, T.H.Barnes, and T.G.Haskell, "Adaptive wave-front correction by means of all-optical feedback interferometry," *Opt. Lett.*, **25**, p.773 (2000).
- 10) M.T.Gruneisen, T.Martinez, D.V.Wick, J.M.Wilkes, J.T.Baker, and I.Percheron, "Holographic Compensation of Severe Dynamic Aberrations in Membrane-Mirror Based Telescope Systems," *Proc.SPIE*, **3760**, p.142 (1999).
- 11) J.Liang, D.R.Williams, and D.T.Miller, "Supernormal vision and high-resolution retinal imaging through adaptive optics," *J. Opt. Soc. Am.*, **A14**, p.2884 (1997).
- 12) J.Gluckstad, "Phase contrast image synthesis," *Opt.Commun.*, **130**, p.225 (1996).
- 13) H.Toyoda, J.Gluckstad, N.Yoshida, and T.Hara, "A Laser Projection System by a Phase Contrast Filtering Employing a Self-Alignment Optical Arrangement," *Kogaku(in Japanese)*, **31**, p.31(2002).
- 14) P.C.Morgensen and J.Gluckstad, "Dynamic array generation and pattern formation for optical tweezers," *Opt.Commun.*, **175**, p.75 (2000).